Quantitative Analyses of High-Resolution 3D MR Images of Highly Myopic Eyes to Determine Their Shapes

Muka Moriyama,[1] *Kyoko Ohno-Matsui,*[1] *Toshio Modegi,*[2] *Junichi Kondo,*[2] *Yoichi Takahashi,*[2] *Makoto Tomita,*[3] *Takashi Tokoro,*[1] *and Ikuo Morita*[4]

Purpose. We analyzed the symmetry and pointedness of the posterior segment of highly myopic eyes.

Methods. We studied 234 eyes of 117 patients with bilateral high myopia (refractive error ≤−8.00 diopters [D]) and 40 eyes of 20 patients with emmetropia (refractive error between −1.0 and +1.0 D). Volume renderings of high-resolution magnetic resonance (MR) images were performed to obtain 3D images of the eye. To analyze the symmetry and pointedness of the posterior surface, a software was developed to measure the area and angle of a fan-shaped segment formed by selected points on the MR images.

Results. All of the emmetropic eyes were symmetrical in the horizontal and sagittal planes with no deformity. In highly myopic eyes, the shape was symmetrical in the horizontal plane in 146 eyes (62.4%) and in the sagittal plane in 162 (69.2%). The shape of the posterior pole was pointed (angle of fan-shaped segment <150°) in 45.7% and blunted (angle ≥150°) in 54.3% of highly myopic eyes. The most common shape was symmetrical in the horizontal and sagittal planes, and the posterior surface was blunt. The shape of the two eyes of the same individual was the same in 61 of 117 patients (52.1%). In 56 patients whose two eyes had different shapes, the most frequent pattern was a difference in the pointedness (51.8%).

Conclusions. Quantitative assessments of the shape of eyes were useful in determining the pattern of eye shape deformity specific to pathologic myopia. (*Invest Ophthalmol Vis Sci.* 2012;53:4510–4518) DOI:10.1167/iovs.12-9426

Pathologic myopia is a major cause of blindness worldwide.[1–3] Eyes with pathologic myopia not only have elongated axial lengths, but also have different shapes.[4,5] Although the elongation of the eye can be measured by laser instruments, for example IOL Master (Carl-Zeiss, Tubingen, Germany), the shape of the eye has been difficult to determine. Examinations of optical coherence tomographic (OCT) images have been useful; however, only a limited area of the posterior segment of the eye can be examined.

We recently studied the shapes of highly myopic eyes with high-resolution magnetic resonance (MR) imaging with volume rendering of the acquired images.[6] We analyzed the 3-dimensional (3D) topographic images of these eyes and showed that the ocular shape of the highly myopic eyes could be classified into 4 distinct types: nasally distorted, temporally distorted, cylindrical, and barrel-shaped.[6] However, the classification of the shape in that study was based on the subjective judgments of the investigators. Such subjective analysis had a risk of misjudging the eye shape between investigators. In addition, because the differences in the shape can be small, such subjective analysis would make it difficult to follow changes in the eye shape of the same individual with increasing time.

To overcome these problems, we developed a computer program to analyze the eye shape of highly myopic patients obtained from the 3D MR images.

Methods

The procedures used in our study adhered to the tenets of the Declaration of Helsinki, and were approved by the Ethics Committee of Tokyo Medical and Dental University. A written informed consent was obtained from all participants.

We studied 117 patients with bilateral pathologic myopia, defined as a refractive error (spherical equivalent) ≤−8.0 diopters (D) or an axial length >26.5 mm. As controls, 20 individuals with emmetropia (refractive error between −1.0 and +1.0 D) were evaluated in the same way. All emmetropic participants were current or former staff members of the University and all volunteered. The clinical characteristics of the participants are shown in Table 1. Patients with a history of scleral buckling or ocular trauma that could affect the eye shape were excluded.

All participants had comprehensive ocular examinations, including the best-corrected visual acuity (BCVA), refractive error measurements, axial length measurements using IOL Master (Carl-Zeiss), visual fields with a Goldmann perimeter, detailed ophthalmoscopic examinations, fluorescein fundus angiography (FFA), and OCT. The refractive status was measured with an autorefractometer (ARK-730; Nidek, Nagoya, Japan) without cycloplegia, and the BCVA was measured with a chart of Landolt rings set at a distance of 5 m. The decimal BCVAs were converted to the logarithm of minimal angle of resolution (logMAR) units for statistical analyses. The correlation between the eye shape and three representative fundus lesions specific to pathologic myopia, that is myopic choroidal neovascularization (myopic CNV), myopic chorioretinal atrophy, and myopic traction maculopathy (MTM), was determined.

A Cirrus OCT (Carl Zeiss Meditec, Oberkochen, Germany) was used to detect the presence of MTM, and FFA and OCT were used to detect the presence of a myopic CNV. Some of the eyes had visual field defects that were not associated with the three myopic lesions. In these eyes, we examined carefully the relationship between the shapes of the eyes

From the Departments of [1]Ophthalmology & Visual Science and [4]Cellular Physiological Chemistry, Tokyo Medical and Dental University Graduate School of Medicine and Dental Sciences, Tokyo, Japan; [3]Clinical Research Center, Tokyo Medical and Dental University Hospital of Medicine, Tokyo, Japan; and [2]Dai Nippon Printing Co., Ltd., Tokyo, Japan.

Submitted for publication January 3, 2012; revised April 3, May 16, and May 29, 2012; accepted May 29, 2012.

Disclosure: **M. Moriyama**, None; **K. Ohno-Matsui**, None; **T. Modegi**, Dai Nippon Printing Co., Ltd. (E); **J. Kondo**, Dai Nippon Printing Co., Ltd. (E); **Y. Takahashi**, Dai Nippon Printing Co., Ltd. (E); **M. Tomita**, None; **T. Tokoro**, None; **I. Morita**, None

Corresponding author: Kyoko Ohno-Matsui, Department of Ophthalmology and Visual Science, Tokyo Medical and Dental University, 1-5-45 Yushima, Bunkyo-ku, Tokyo 113, Japan; k.ohno.oph@tmd.ac.jp.

Investigative Ophthalmology & Visual Science, July 2012, Vol. 53, No. 8

Table 1. Patient and Study Eye Characteristic at the Initial Examination

	High Myopia	Emmetropia
Sex. No. patients (eyes)		
Men	24 (48)	11 (22)
Women	93 (186)	9 (18)
Age (y), mean ± SD	60.0 ± 12.3	52.7 ± 13.2
Refractive error (D), mean ± SD	−15.5 ± 6.1	0.06 ± 0.63
Axial length (mm), mean ± SD	30.3 ± 2.3	23.3 ± 0.7
Baseline logMAR, mean ± SD	0.33 ± 0.48	0.02 ± 0.03

and the visual field defects. The visual fields were quantified by using a grid system proposed by Kwon et al.[7] The grid consisted of 100 sectors that lay within the V4 isopters. The visual field score ranged from 0 (total loss of vision within the V4 isopter) to 100 (normal visual field). We considered eyes with a loss in >10% of the dots to have significant visual field defects as we have reported previously.[8]

MR Imaging

MR imaging examinations and volume rendering of MR images of the eyes were done as reported previously.[6] All patients were examined with a whole-body MR scanner (Signa HDxt 1.5T, version 15; GE Healthcare, Waukesha, WI). To obtain a high-contrast delineation of the border of the eye, the following scanning sequence was performed: fat-suppressed T2-weighted cube, which is an improved sequence of 3D-fast-spin-echo (3DFSE), with the parameters of 256 × 256 matrix, 22 cm field of view, 1.2-mm slice thickness, repetition time (TR) 2500 ms, echo time (TE) 90 ms, and echo train length (ETL) 90. The scan time for each subject was 4 minutes. T2-weighted MRI, which images the intraocular fluid and not the sclera, was used.

Volume renderings of the images were done on a computer workstation (version AW 4.4; GE Healthcare) to obtain high-resolution 3D data. The borders of the globe were identified semi-automatically by the signal intensity, and the tissues on the outside of the globe were removed. The boundary between the retina and vitreous fluid was determined by adjusting the signal intensity in the volume rendering of the MR images. When the signal intensity gradually was increased manually, only the signal from vitreous fluid remained. De-noising, such as smoothing or curve/surface fitting, was done automatically by the computer workstation after the volume rendering of the images was done.

Establishment of Central Axis Line

First, the center of gravity (Pg) was determined by the coordinates of the contour of the shape. Then, one point on the anterior edge of the eye was defined (Pa). Initially, Pg was fixed, and Pa was shifted along the anterior border. Then one point (Pc) on the Pg-Pa line was defined, and Pc was moved to several locations from Pb to Pa in one-pixel steps. The intersection point of the contour and the line crossing orthogonally to Pg-Pa on Pc was defined as P_{+v} and P_{-v}, respectively. Pa was calculated to be when the difference between the length of Pc-P_{+v} and the length of Pc-P_{-v} at each Pc point became a minimum. After the correction of Pa, Pa was fixed and Pg was shifted by changing the Y-coordinate. Any one point (Pc) on the Pg-Pa axis was defined, and then Pg was recalculated in the same way. After the correction of Pa and Pg, the Pa-Pg line was set to be central axis line (Supplementary Figs. 1–6, http://www.iovs.org/lookup/suppl/doi:10.1167/iovs.12-9426/-/DCSupplemental).

Measurement of Eye from 3D MR Image

The views of the eye from 6 directions (anterior, posterior, superior, inferior, nasal, and temporal) were incorporated into the software of the 3D MR image (Fig. 1). A central axis line was drawn automatically through the eye. The following parameters were measured in pixels automatically by the software:

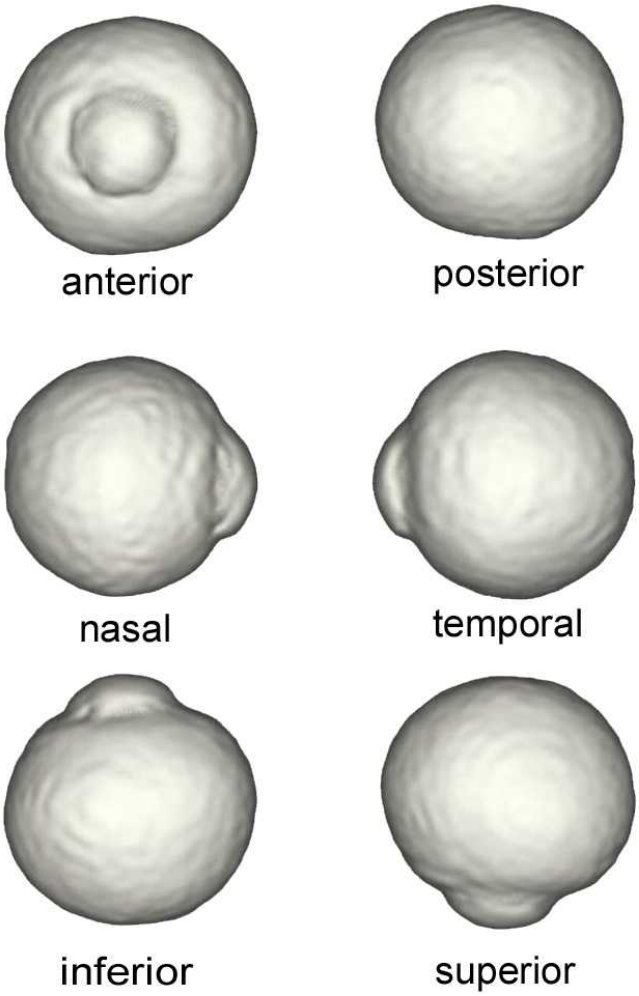

Figure 1. The 6 views of the eye that were analyzed by our software. These views are those of a 3D MR image.

1. Sagittal axial length: Length of central axis (Figs. 2, 3; red dotted line).
2. Vertical length of eye: Length of line that crosses orthogonally to the central axis at the midpoint of the sagittal line (Fig. 3B, blue dotted line).
3. Horizontal length of eye: Length of a line that crosses orthogonally to the central axis at its midpoint in the horizontal plane (Fig. 3A, blue dotted line).
4. Posterior basal point (Pb): Point of intersection of the central axis and the posterior edge of the eye.
5. Point of origin (Po): Point on the central axis 87 pixels anterior to Pb, which is approximately 12.5 mm from Pb. This is different from the midpoint of the central axis and was done to avoid the influence of the axial length on the location of Po.
6. P_{+n}: Point on the posterior surface of the eye that is 22.5° nasal (in horizontal plane) or inferior (in sagittal plane) to Po.
7. P_{-n}: Point on the posterior surface of the eye that is 22.5° temporal (in horizontal plane) or superior (in sagittal plane) to Po.
8. P_{+w}: Point on the posterior surface that is 45° nasal (in horizontal planes) or inferior (in sagittal planes) to Po.
9. P_{-w}: Point on the posterior surface that is 45° temporal (in horizontal planes) or superior (in sagittal planes) to Po (Figs. 2, 3).

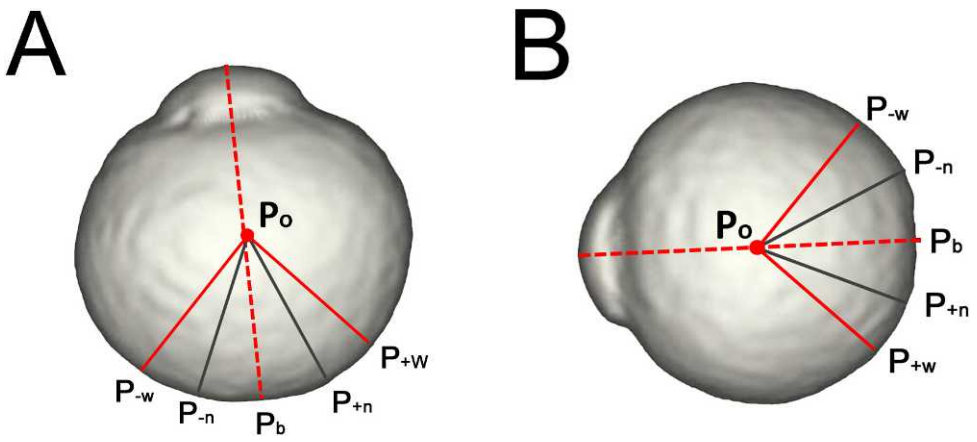

Figure 2. The central axis line is drawn automatically (*red dot line*), and the measurement points (P_b, P_o, $P_{\pm n}$, $P_{\pm w}$) also are set automatically. (**A**) Horizontal plane. (**B**) Sagittal plane.

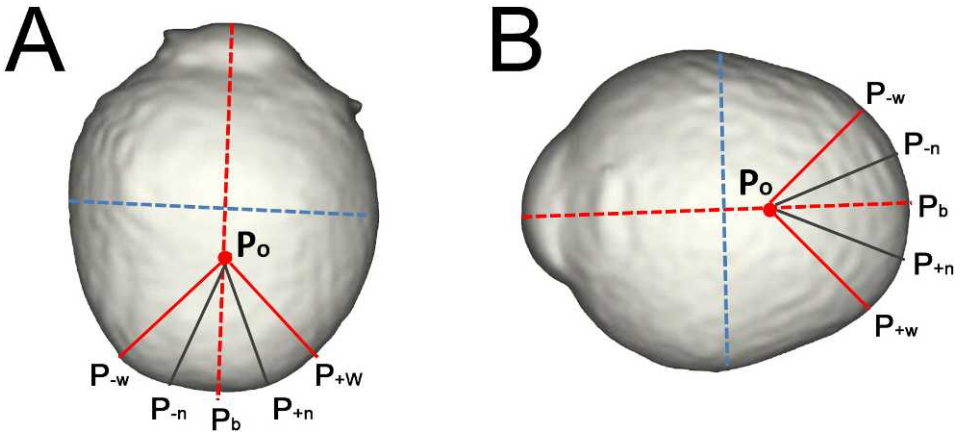

Figure 3. The central axis line is drawn automatically (*red dot line*), and the measurement points (P_b, P_o, $P_{\pm n}$, $P_{\pm w}$) also are set automatically. (**A**) The vertical length is shown (*blue dotted line*). (**B**) The horizontal length is shown (*blue dotted line*).

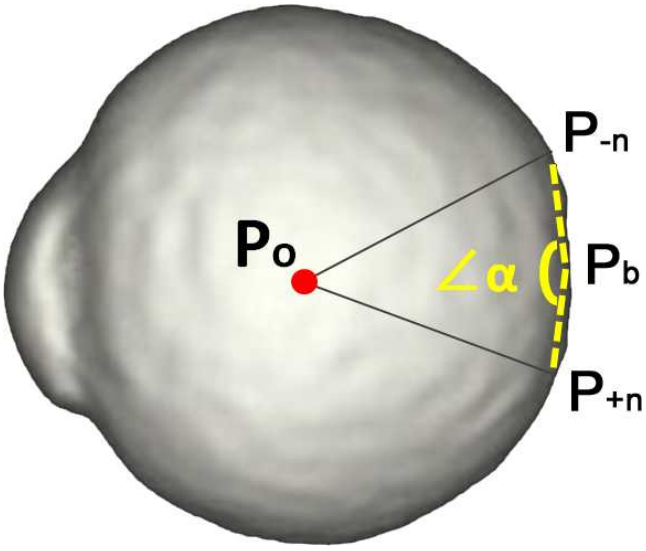

Figure 4. The pointedness of the posterior surface is represented by the angle formed by P_{+n}, $-P_b$, and P_{-n} ($\angle\alpha$). The angle was measured for 4 views (nasal, temporal, inferior, superior), and the mean value was adopted as the pointedness of the posterior surface.

The area (in pixels) of the fan-shaped segment formed by Po, Pb, and P_{+n} was defined as S_{+n}, and the segment formed by Po, Pb, and P_{+w} was defined as S_{+w}. S_{-n} and S_{-w} were defined similarly.

Based on these landmarks, the following parameters were calculated and used for the statistical analyses: Ratio of the vertical length to axial length (V/A ratio), ratio of the horizontal length to axial length (H/A ratio), and degree of symmetry of the posterior surface of the eye. The degree of symmetry in the horizontal plane was determined by the ratio of the area of the temporal segment to that of the nasal segment (T/N ratio). $S_{+w} \times 100/S_{-w}$ in the horizontal plane was defined as a wide T/N ratio, and $S_{+n} \times 100/S_{-n}$ as a narrow T/N ratio. For wide and narrow T/N ratios, the ratios that were more apart from 100 were chosen. The eyes whose T/N ratio was >110 were classified as having a temporally-distorted shape, and the eyes whose T/N ratio was <90 were classified as having a nasally-distorted shape. Eyes whose T/N ratio was between 90 and 110 were classified as horizontally symmetrical.

The degree of symmetry in the sagittal plane was determined by the ratio of the area of the superior segment to that of the inferior segment (S/I ratio). $S_{+w} \times 100/S_{-w}$ in the sagittal plane was defined as a wide superior-to-inferior ratio (S/I ratio), and $S_{+n} \times 100/S_{-n}$ as a narrow S/I ratio. For wide and narrow S/I ratios, the ratio that was more apart from 100 was chosen to represent the symmetry in the sagittal plane. The eyes whose S/I ratio was >110 were classified as superior-distorted shape, and the cases whose S/I ratio was <90 were classified as inferior-distorted shape. The cases whose S/I ratio was between 90 and 110 were classified as sagittally symmetrical.

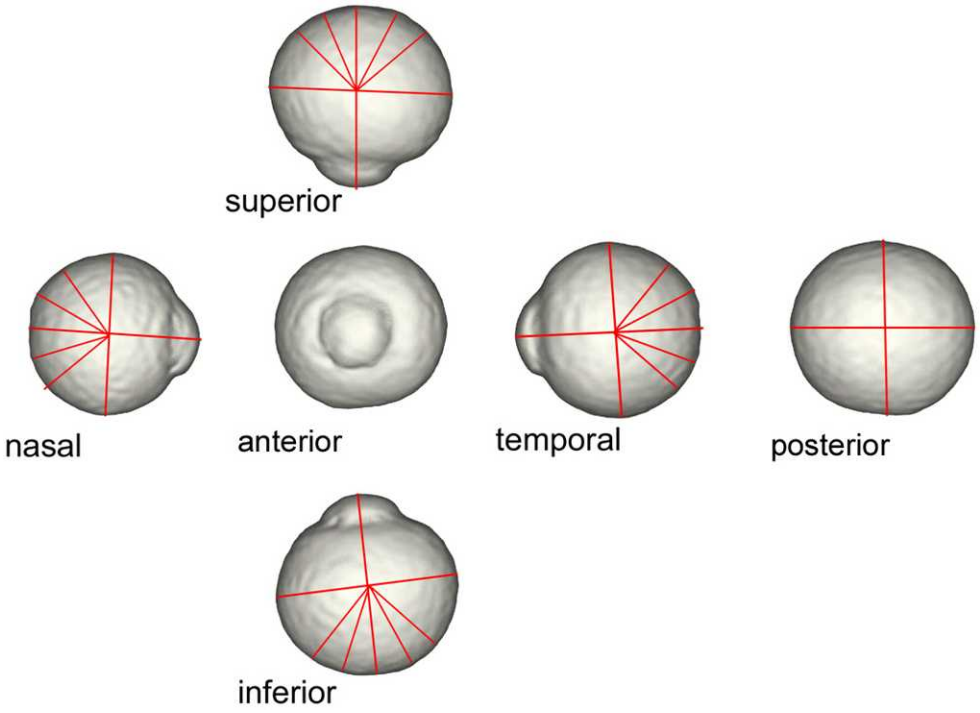

Figure 5. The right eye of a 61-year-old man with emmetropia (axial length 24.8 mm). The V/A ratio is 95, the H/A ratio is 100, the T/N ratio is 98, the S/I ratio is 102, and the pointedness is 162. These data indicated that the eye is blunt with no deformities.

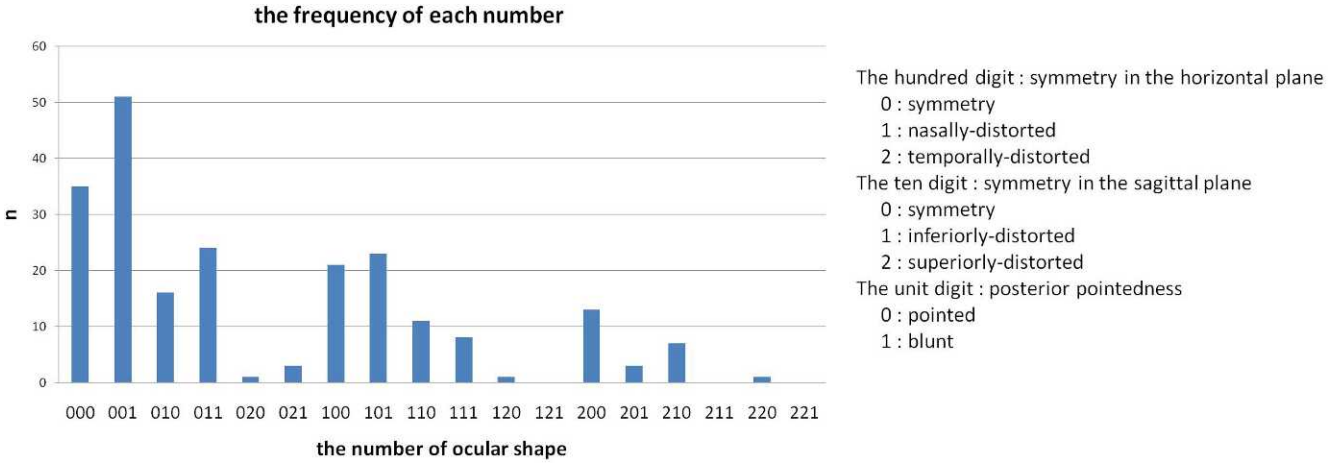

Figure 6. Bar graph showing the frequency of the different types of ocular deformities. The most frequent type is 001, and the second most frequent type is 000.

We also calculated the shape of the posterior surface. The angle ($\angle$) formed by P_{+n}-P_b-P_{-n} was defined as the posterior pointedness (Fig. 4). The shape of the posterior segment of the globe was defined as "pointed" when this angle was $<150°$ and "blunt" when this angle was $\geq 150°$.

Deformities of Eye

When an eye was spherical, the V/A and H/A ratios were approximately 100. We defined eyes as not being deformed when the V/A and H/A ratios were both >95.

For the eye whose V/A or H/A ratio was ≤ 95, the deformity of the eye was expressed by a three-digit figure, where the hundreds digit represented the symmetry in the horizontal plane (symmetrical = 0, nasally-distorted = 1, and temporally-distorted = 2), the tens digit represented the symmetry in the sagittal plane (symmetrical = 0, inferiorly-distorted = 1, superiorly-distorted = 2), and the unit digit represented the pointedness of the posterior segment of the eye (pointed = 0, blunt = 1).

The eyes were classified finally into the 18 types according to the different combinations of these figures from 000–221 (Table 2).

Statistical Analyses

The significance of the differences in patients' age, BCVA, axial length, and the parameters of deformities was determined by Student's *t*-tests, Welch's *t*-tests, Mann-Whitney's *U* test and the Kruskal-Wallis test. The frequency of ocular deformity, visual field defects, MTM, CNV, and chorioretinal atrophy was compared using the χ^2 test. The correlation between posterior pointedness and age or axial length was analyzed by

Table 2. Summary of 18 Types of Eye Shape

Number	Symmetricity		Shape of Posterior Surface
	In Horizontal Plane	In Sagittal Plane	
000	Symmetrical	Symmetrical	Pointed
001	Symmetrical	Symmetrical	Blunt
010	Symmetrical	Inferiorly-distorted	Pointed
011	Symmetrical	Inferiorly-distorted	Blunt
020	Symmetrical	Superiorly-distorted	Pointed
021	Symmetrical	Superiorly-distorted	Blunt
100	Nasally-distorted	Symmetrical	Pointed
101	Nasally-distorted	Symmetrical	Blunt
110	Nasally-distorted	Inferiorly-distorted	Pointed
111	Nasally-distorted	Inferiorly-distorted	Blunt
120	Nasally-distorted	Superiorly-distorted	Pointed
121	Nasally-distorted	Superiorly-distorted	Blunt
200	Temporally-distorted	Symmetrical	Pointed
201	Temporally-distorted	Symmetrical	Blunt
210	Temporally-distorted	Inferiorly-distorted	Pointed
211	Temporally-distorted	Inferiorly-distorted	Blunt
220	Temporally-distorted	Superiorly-distorted	Pointed
221	Temporally-distorted	Superiorly-distorted	Blunt

Spearman's correlation coefficient rank test. A value of $P < 0.05$ was considered statistically significant.

Results

Eye shape was analyzed by our software successfully in all of the eyes. The time required for the analysis of each 3D MR image was approximately one second. The repeatability of the analysis by the software was confirmed by measuring the parameters of the 3D-MR images taken at different times in 2 individuals, and the results were exactly the same.

Analysis of Emmetropic Eyes

The mean V/A ratio of emmetropic eyes was 99.5 ± 3.5 (range 95.0–104.5) and the mean H/A ratio was 101.2 ± 3.4 (range 95.5–105.0). These data indicated that the axial, vertical, and horizontal lengths were approximately the same, and the shape of emmetropic eyes was spherical. The average T/N ratio was 96.9 ± 4.6 (range 91.0–105.0) and the average S/I ratio was 93.3 ± 3.8 (range 91.0–102.0). The average pointedness of the posterior surface of emmetropic eyes was 157.5 ± 4.4 (range 150–163).

Thus, the shape of emmetropic eyes was symmetrical in the horizontal and sagittal planes, and the posterior shape was calculated to be blunt (Fig. 5). None of the emmetropic eyes had a deformity of the eye shape according to our definition, and the three digit score was 001.

Analysis of Eyes with Pathologic Myopia

In eyes with pathologic myopia, the T/N ratio ranged from 90–110 in 146 of 234 eyes (62.4%), and thus the posterior surface of these eyes was symmetrical in the horizontal plane. A nasally-distorted shape with a T/N ratio <90 was found in 64 eyes (27.4%) and temporally-distorted shape with a T/N ratio >110 was found in 24 eyes (10.3%).

In the sagittal plane, the posterior eye surface was symmetrical, with an S/I ratio of 90–110 in 162 of 234 eyes (69.2%). An inferiorly-distorted shape with an S/I ratio <90 was found in 66 eyes (28.2%), and only 6 eyes (3%) had a superiorly-distorted shape with an S/I ratio >110.

Of 234 eyes 107 (45.7%) had a pointed posterior surface with a P_{+n}-P_b-P_{-n} angle that was <150 degrees, and 127 eyes (54.3%) had a blunt surface with the P_{+n}-P_b-P_{-n} angle that was ≥150 degrees. The P_{+n}-P_b-P_{-n} angle was significantly smaller in the temporally-distorted eyes than in the nasally-distorted eyes or the horizontally-symmetrical eyes (142.5 ± 7.1, 149.2 ± 8.0, and 152.4 ± 8.8, respectively; $P = 1.54 \times 10^{-4}$, Kruskal-Wallis test).

As opposed to the emmetropic eyes, only 6/234 eyes (2.6%) among the 3 highly myopic patients had a V/A and H/A ratio >95. This indicated that they had no deformity in the eye shape. These 3 patients were significantly younger and had shorter axial lengths than the other 114 highly myopic patients (mean age 40.0 ± 6.1 vs. 60.6 ± 12.0 years, $P = 0.01$; and mean axial length 27.9 ± 1.0 vs. 30.3 ± 2.3 mm, $P = 0.005$, Mann-Whitney's U test).

The eye shapes were analyzed further in the remaining 114 highly myopic patients (93.2%). The frequency of the different eye shapes as expressed by the three-digit figure is shown in Figure 6. The most frequent type was 001, in which the eyes were symmetrical in the sagittal and horizontal planes, and the posterior pole was blunt (Fig. 7). This type was found in 51 of 228 eyes (23.4%). The second most frequent type was 000, in which the eye was symmetrical in the sagittal and horizontal planes, and the posterior pole was pointed (Fig. 8). This type was found in 35 of the 228 eyes (16.1%).

The type of eye shape was the same in both eyes of an individual in 61 of 117 highly myopic patients (52.1%), and was different in the remaining 56 patients. The average difference in the axial lengths between the two eyes was 1.35 ± 1.37 mm in the patients who had different shapes in the two eyes. This was significantly higher than that in patients whose eye shape was the same in both eyes (0.86 ± 0.76 mm, $P = 0.02$, Welch's t-test).

In the 56 patients whose two eyes had different shapes, the most frequent pattern of the difference was that for the pointedness of the posterior pole of the eye (the unit digit) in 29 patients (51.8%). The second most frequent pattern was for eyes that were symmetrical in the sagittal plane (the tens digit), and this was found in 25 patients (44.6%). These were followed by the difference in the degree of symmetry in the horizontal plane (the hundreds digit) in 19 patients (33.9%). The most common pair of figures in the patients who had different shapes in both eyes was the pair of "100" and "101." This pair was found in 6 of 56 patients (10.7%). The details of the pairs are shown in Supplementary Table 1 (http://www.iovs.org/lookup/suppl/doi:10.1167/iovs.12-9426/-/DCSupplemental).

All of the digits were different in 2 patients, the unit and tens digits were different in 5, the unit digit and hundreds digit were different in 6, and the tens and hundreds digits were different in 2.

Correlation between Type of Eye Shape and Axial Length and Age

We calculated the correlation between the age of the patient and the eye shape in 61 highly myopic eyes whose eye shape was the same in both eyes. There was no correlation between age and the degree of symmetry in the horizontal plane (T/N ratio), or between age and the degree of symmetry in the sagittal plane (S/I ratio). However, there was a significant negative correlation between the degree of pointedness of the eye and the patients' age ($r = -0.38$, $P = 0.003$, Spearman's correlation coefficient by rank test, Fig. 9).

There was no significant correlation between the axial length and any of the parameters (pointedness, degree of

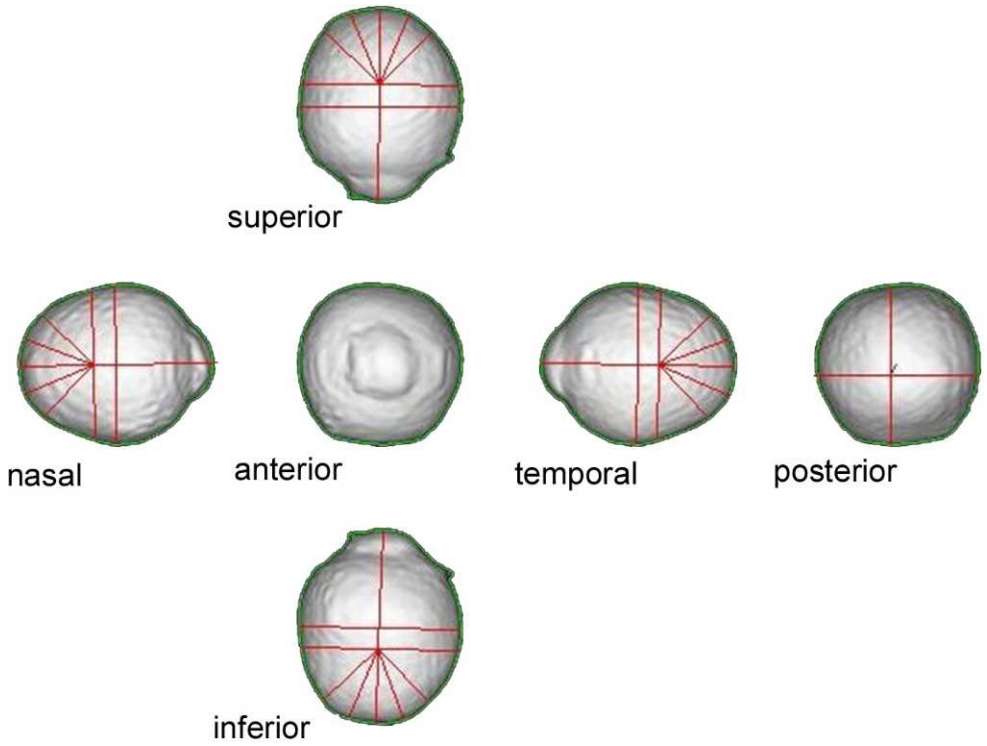

Figure 7. The left highly myopic eye of a 60-year-old man (axial length 33.1 mm). The V/A ratio is 81.5, the H/A ratio is 83, the T/N ratio is 96, the S/I ratio is 94, and the pointedness is 159. These data indicate that the type of ocular shape is 001.

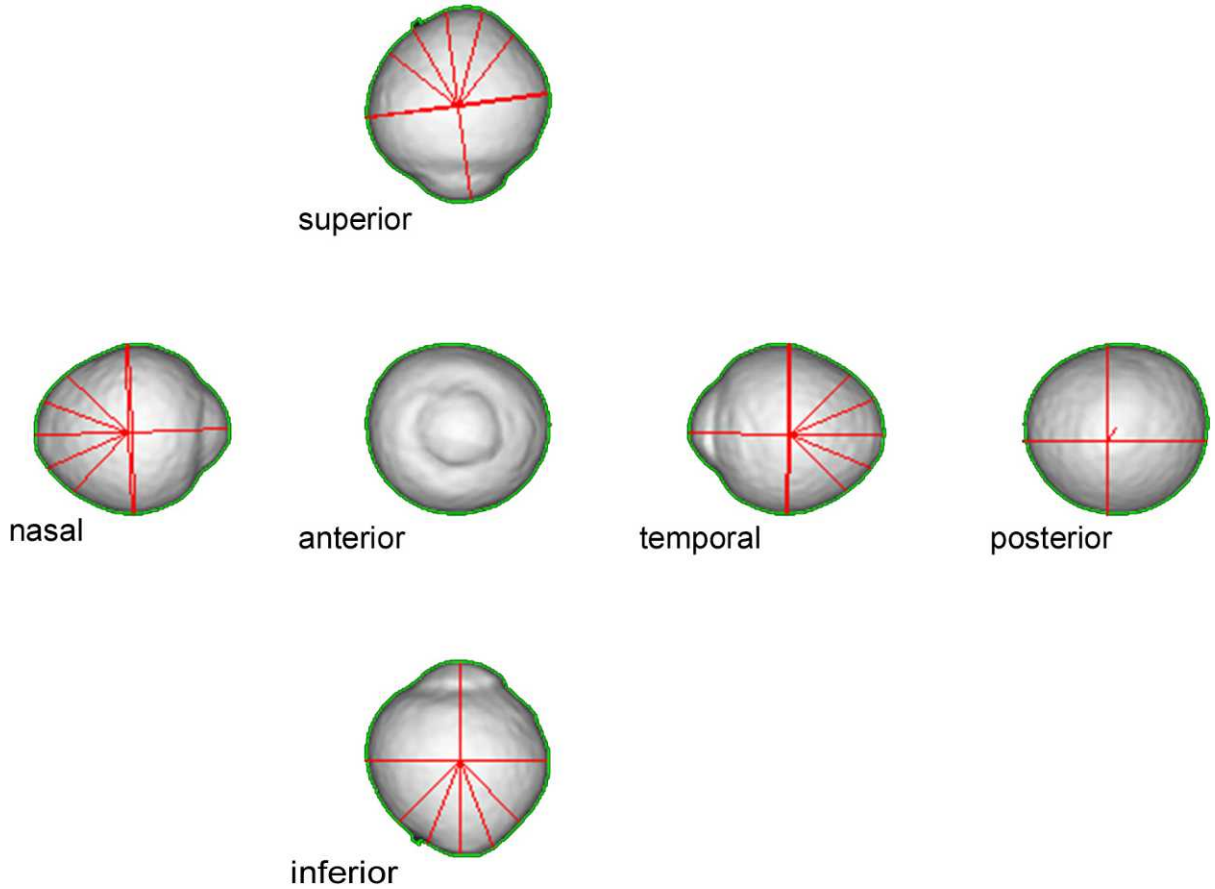

Figure 8. The highly myopic left eye of a 32-year-old woman (axial length 26.6 mm). The V/A ratio is 85.5, the H/A ratio is 92.5, the T/N ratio is 103, the S/I ratio is 95, and the pointedness is 147. These data indicate that the type of ocular shape is 000.

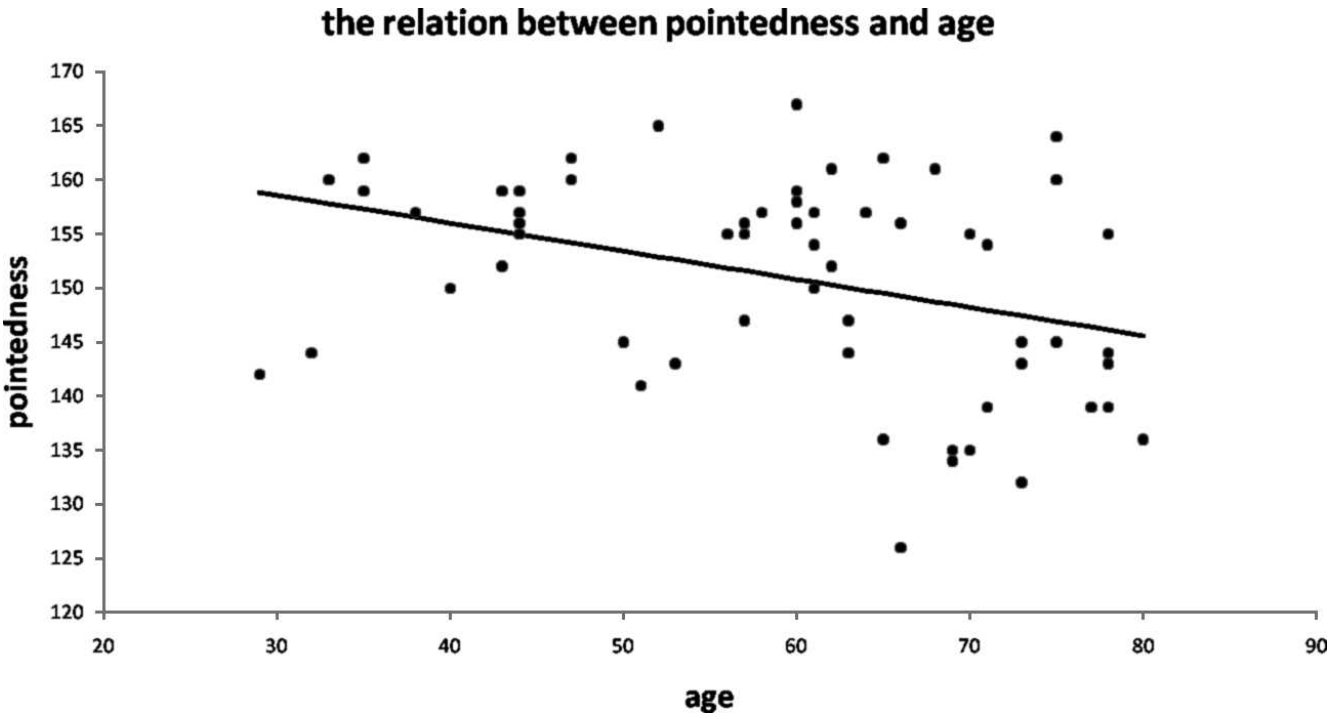

FIGURE 9. Graph showing the relationship between the degree of pointedness and the age. There was a significant negative correlation between the degree of pointedness of the eye and the patients' age ($r = -0.38$, $P = 0.003$).

symmetry in the horizontal plane, and degree of symmetry in the sagittal plane). When we divided the eyes into 2 groups according to the axial length (those with an axial length $\geq$30.0 mm [120 eyes] and those with an axial length <30.0 mm [114 eyes]), the number of 2's in the hundreds digit (the temporally-distorted shape) was found significantly more frequently in the eyes with a longer axial length (14.2%, 17 of 120 eyes) than in the eyes with a shorter axial length (6.1%, 7 of 114 eyes, $P = 0.04$, χ^2 test).

Association between Deformity or Symmetry and Fundus Lesions Specific to Pathologic Myopia

We examined the frequency of MTM, CNV, and chorioretinal atrophy among the different figures in each digit. The frequency of CNV was not associated significantly with the figure of each digit. On the other hand, the MTM and myopic chorioretinal atrophy were present significantly less frequently in the eyes with 0 in hundreds digit, which represents the horizontal symmetry ($P = 0.005$ and 0.04, respectively; χ^2 test), and were present significantly more frequently with a 0 in the ones digit, which is related to the pointedness of the posterior surface ($P = 4.9 \times 10^{-5}$ and 0.03, respectively; χ^2 tests).

Effects of Deformity and Symmetry on Visual Function

We then determined the absolute value of asymmetry and analyzed the effect of asymmetry on visual function. The absolute value of horizontal asymmetry was defined as the difference between T/N ratio and 100, and the absolute value of sagittal asymmetry was defined as the difference between S/I ratio and 100. Asymmetry in the horizontal and sagittal planes was not correlated significantly with the BCVA. However, the horizontal asymmetry was significantly higher in the eyes with significant visual field defects than in eyes without visual field defects ($P = 0.02$, Welch's *t*-tests). The visual defects were detected significantly more frequently with the number 2 in the hundreds digit, which represents temporally distorted eyes ($P = 2.2 \times 10^{-5}$, χ^2 test). The correlations between the asymmetry of the eye and patients' age or axial length were not significant.

Discussion

Our results showed that our software can analyze successfully the 3D MR images of eyes quantitatively and objectively within 1 second per eye. This makes it practical to compare the eye shapes among different populations or ethnicities, and also makes it possible to follow the changes in the shape of human eyes longitudinally.

None of the emmetropic eyes met the definition of being deformed by our software analyses. In the emmetropic eyes, the axial, vertical, and horizontal lengths were not significantly different. Also, the shape of the posterior surface of the eye was symmetric horizontally and sagittally, and was classified as being blunt. Thus, we conclude that the shape of emmetropic eyes is spherical.

In contrast to the emmetropic eyes, only 2.6% of the eyes with pathologic myopia were analyzed to have no deformity by our software. The highly myopic patients whose eyes had a deformity were significantly older and had significantly longer axial lengths than those whose eyes did not have a deformity. This suggests that the deformity of the eyes with pathologic myopia increases as the patient ages, which agrees with the findings in an earlier study on highly myopic eyes observed by stereoscopic fundus examinations.[9] However, this must be confirmed in a future study with a larger number of eyes.

In the sagittal plane, 69.2% of the highly myopic eyes had a symmetric posterior surface. Of the 72 eyes whose posterior eye shape was not symmetric in the sagittal plane 66 (91.7%) had an inferiorly-deformed shape and only 8.3% had a superiorly-deformed shape. In our earlier study, we examined

the 3D MR image from the nasal side and judged the shape of the eye subjectively.[6] In that study, the part of the eye that most protruded existed along the visual axis in 78.3% of the myopic eyes, and all of the remaining eyes had the most protruded part inferior to the central axis. In our present study, the percentage of the eyes whose posterior eye shape was symmetric sagittally was slightly lower than that in our previous study,[6] and a superiorly-deformed type, which was not found in our earlier study, was identified. This difference was most likely because the current study was more quantitative and more detailed analyses of the 3D MR images were made by our software. We also had a larger number of patients.

Our results confirmed that a posterior bulge, if it existed, developed inferior to the central axis much more frequently than superior to the central axis. Very recently, Tanabe et al. reported that the choroid inferior to the optic disc was significantly thinner than that in the other sectors around the optic disc in 28 eyes with no ocular pathologies (mean refractive degree -3.6 ± 4.1 D).[10] They suggested that the thinner choroid inferior to the optic disc may be a natural anatomic architecture of normal eyes. Although it was not determined if the sclera inferior to the optic disc was thinner than other areas in normal eyes, their data in combination with our results suggest that the inferior fundus already is thinner in normal eyes and, thus, might be more susceptible to expansion in response to intraocular pressure in pathologic conditions, such as pathologic myopia or tilted disc syndrome. The precise mechanism for this phenomenon must be determined in the future.

We found that 62.4% of the highly myopic eyes were symmetric in the horizontal plane, 27.4% were nasally-distorted, and 10.3% were temporally-distorted. In our earlier study, we classified the eye shape into 4 different types (temporally-distorted, nasally-distorted, cylindrical, and barrel-shaped) based on an inferior view.[6] In that study, 36.7% had the nasally-distorted type and 16.7% had the temporally-distorted shape. Although the incidence of nasally-distorted or temporally-distorted eyes was slightly lower than that found in our current study, the difference between the two studies was not significant.

Our analyses showed that all of the emmetropic eyes had a blunt shape. Among the highly myopic eyes, on the other hand, as many as 45.7% were classified as being pointed. In addition, there was a significant negative correlation between the degree of pointedness and the patients' age (Fig. 9). This suggested that an increase in the pointedness of the posterior surface of the eye might be one important feature of eyes with pathologic myopia, and this becomes more evident as the patients age.

After classifying the eye shape into 18 types by our software, the eye shape was identical in 52.1% of highly myopic patients. This rate was lower than that of 69.8% in our previous study,[6] which probably is due to the more quantitative classification in the present study.

In patients whose eye shape was not identical between the two eyes of the same individual, the most frequent pattern of differences was the degree in the pointedness of the posterior surface of the eye. This suggests that the pointedness may be altered more easily in highly myopic eyes than the degree of horizontal or sagittal symmetry.

Finally, we calculated the absolute value of the asymmetry of the eyes and examine whether the degree of asymmetry was significantly correlated with visual function. Statistical analyses showed that the horizontal asymmetry was significantly higher in the eyes with significant visual field defects than the eyes without visual field defects. Our previous study showed that significant visual field defects were found significantly more frequently in eyes with a temporally-distorted shape.[6] Also, multiple linear regression analyses of a more recent set of data showed that the presence of an abrupt change of the scleral curvature temporal to the optic disc was the only factor associated significantly with a progression of the visual field defects.[8] These results, combined with our present data, suggest that horizontal asymmetry of the posterior surface of the eye might be a cause of optic nerve damage.

Our results also showed that the degree of pointedness was associated significantly with the degree of horizontal symmetry. The absolute value of pointedness of the posterior eye surface was significantly greater in eyes with a temporally-distorted shape than in the nasally-distorted type or horizontally-symmetrical eyes. Also, the MTM and myopic chorioretinal atrophy were present significantly less frequently in horizontally-symmetrical eyes and more frequently in eyes classified as being pointed. These findings suggested that an increased horizontal asymmetry and increased pointedness of the posterior surface shape of highly myopic eyes might be important factors that might cause the development of most of the vision-threatening complications specific to pathologic myopia, regardless of whether they develop in the papillary or macular region. A more precise mechanism of how specific types of changes in the eye shape are related to the development of myopic pathologies must be determined in a larger number of eyes with a longer follow-up period.

Our study has some limitations. This was a hospital-based study and the patients studied visited the High Myopia Clinic. Thus, it is possible that more myopic patients with vision difficulties were enrolled than existed in the general myopic population. Also, T2-weighted MRI was used, which images the intraocular fluid and not the sclera. Also, there were no follow-up data. Finally, we did not analyze the anterior portion of the eye. Thus, it is not clear whether such deformities are observed only in the posterior segment of the eye or the anterior segment of the eye also is deformed. This will be investigated in the future.

Despite these limitations, we believe that the analyses of the eye shapes with our software provided more precise and more detailed evaluations of highly myopic eyes. Further studies investigating the characteristics of human eyes, and how they are deformed in high myopes are planned. The effect of age on the eye shape, and the specific types of deformities that are correlated significantly with the vision-threatening complications of highly myopic eyes are ongoing in our institution.

Acknowledgments

Duco Hamasaki assisted with critical discussion and final manuscript revision.

References

1. He M, Zeng J, Liu Y, Xu J, Pokharel GP, Ellwein LB. Refractive error and visual impairment in urban children in southern china. *Invest Ophthalmol Vis Sci*. 2004;45:793–799.
2. Vitale S, Sperduto RD, Ferris FL 3rd. Increased prevalence of myopia in the United States between 1971–1972 and 1999–2004. *Arch Ophthalmol*. 2009;127:1632–1639.
3. Vongphanit J, Mitchell P, Wang JJ. Prevalence and progression of myopic retinopathy in an older population. *Ophthalmology*. 2002;109:704–711.
4. Logan NS, Gilmartin B, Wildsoet CF, Dunne MC. Posterior retinal contour in adult human anisomyopia. *Invest Ophthalmol Vis Sci*. 2004;45:2152–2162.
5. Atchison DA, Pritchard N, Schmid KL, Scott DH, Jones CE, Pope JM. Shape of the retinal surface in emmetropia and myopia. *Invest Ophthalmol Vis Sci*. 2005;46:2698–2707.

6. Moriyama M, Ohno-Matsui K, Hayashi K, et al. Topographic analyses of shape of eyes with pathologic myopia by high-resolution three-dimensional magnetic resonance imaging. *Ophthalmology*. 2011;118:1626–1637.
7. Kwon YH, Kim CS, Zimmerman MB, Alward WL, Hayreh SS. Rate of visual field loss and long-term visual outcome in primary open-angle glaucoma. *Am J Ophthalmol*. 2001;132:47–56.
8. Ohno-Matsui K, Shimada N, Yasuzumi K, et al. Long-term development of significant visual field defects in highly myopic eyes. *Am J Ophthalmol*. 2011;152:256–265.
9. Hsiang HW, Ohno-Matsui K, Shimada N, et al. Clinical characteristics of posterior staphyloma in eyes with pathologic myopia. *Am J Ophthalmol*. 2008;146:102–110.
10. Tanabe H, Ito Y, Terasaki H. Chorid is thinner in inferior region of optic disks of normal eye. *Retina*. 2012;32:134–139.